Defence Science Journal, Vol. 63, No. 4, July 2013, pp. 346-354, DOI : 10.14429/dsj.63.4207

Real Time Mid-course Maneuver and Guidance of a Generic Reentry Vehicle

Avinash Chander* and I.V. Muralikrishna#

*Defence Research and Development Organisation, New Delhi-110 001, India
#Jawaharlal Nehru Technological University, Hyderabad-500 085, India
*E-mail: chander_avinash06@yahoo.co.in

ABSTRACT

The aim of any mission is to accomplish the final objective with desired accuracy and the same is valid for a generic launch vehicle. In many missions it is necessary to execute mid-course maneuvers with an intentional diversion trajectory to create a counter measure or to avoid certain specific known geographical locations. The current work elaborates a novel and practically implementable mid-course maneuver and an ascent phase guidance of a reentry vehicle executing an in-flight determined mid-course maneuver (trajectory reshaping) without compromising the accuracy of the final achieved target position. The robustness of the algorithm is validated with 6DoF simulation results by considering the dispersion of the burnout state vector conditions which arises due to variations in thrust profile, aerodynamics characteristics of the vehicle, atmosphere, etc.

Keywords: Ascent phase guidance, mid-course maneuver, reentry vehicle, terminal accuracy, range augmentation, trajectory reshaping.

1. INTRODUCTION

The primary objective of any launch vehicle is to deliver the Payload to the desired target within the given tolerance bounds. Since the first use of ballistic missile in 1940's, a lot of innovation has gone in the development of more sophisticated guidance, control, navigation algorithm's to enhance the range, accuracy, reliability, etc., In view of the current working scenario there is a demand for the maneuver during flight (trajectory reshaping) such that the mission objectives are achieved without any compromise on the mission end objective. A typical in-flight mid-course maneuver scenario is shown in Fig. 1, where the trajectory in blue color is the one which is going to be followed by the vehicle if there is no intentional maneuver (non-maneuvering) is executed on board and the trajectory in green color is the intentional maneuver trajectory which is hard to predict as compared to the non-maneuvering trajectory.

A reentry vehicle approaches at a very high velocity, typical velocities varying from 5 Km/s - 7 Km/s based on the selected trajectory, downrange, guidance mechanism employed in the design procedure[1]. But with growth of computing power, more powerful and reliable estimation (prediction) and filtering techniques are available today by virtue of which it is possible to predict the trajectory of the reentry vehicle well ahead and take some advance corrective measures.

Optimization based trajectory planning and tracking the reference trajectory using dynamic inversion guidance laws are proposed by Ran[2], *et al.* In the paper the author describes the re-

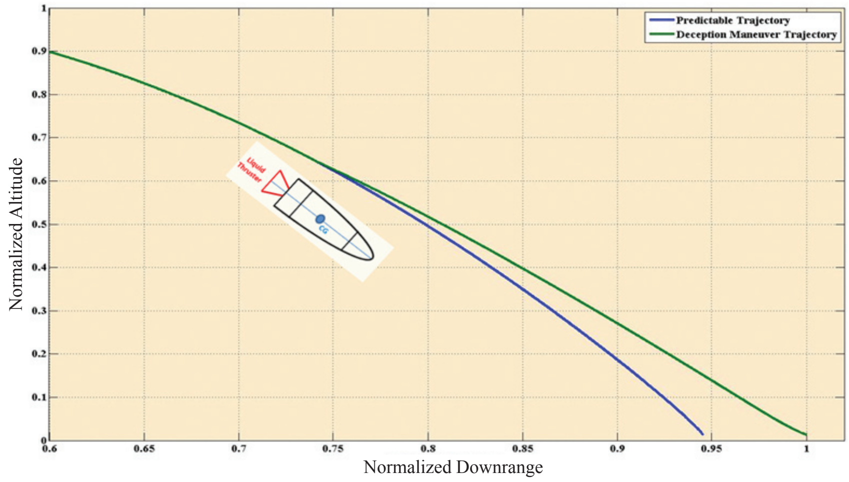

Figure 1. Normalized trajectory of a non-maneuvering and maneuver vehicle.

Received 19 March 2013, revised 14 May 2013, online published 19 July 2013

entry vehicle trajectory planning and guidance by considering the path constraints like aerodynamics heating, aerodynamic load, etc., in r-V plane with an aero assisted configuration. Gao Changsheng[3], *et al*. describes a virtual displacement concept based reentry vehicle guidance using optimization technique and LQG based tracking of the reference trajectory. Page & Rogers[4] summarizes a few investigations carried out in guidance and control of maneuvering reentry vehicles by considering cross-product, proportional and tangent cubic guidance mechanisms having cruciform, bank to turn and fixed trim control configurations.

Explicit re-entry guidance equations for maneuvering re-entry vehicles (MaRVs) using characteristic curve approach is developed Cameron[5]. While formulating the guidance it is ensured that terminal trajectory constraints on path angles and lift acceleration and its derivatives are achieved. Variable gain vector guidance equations are established by forcing terminal equation structure to be similar to the characteristic curve equations. But the study doesn't consider the limitation on aerodynamic capability, maximum acceleration limit nor did an energy management requirement and it assume that this type of characteristic curve calls for less acceleration for large range to go than that for small range to go.

A practically implementable algorithm described in the current paper describes methodology to execute the in-flight determined maneuver of the vehicle and to guide the vehicle in the ascent phase to its predetermined target accurately with in the desired tolerance bounds. The basis of the current approach relies on the capability of simulating the real time scenario of the vehicle dynamics in the background simulation from the burnout point[6,7] to the desired target point.

2. DESIGN METHODOLOGY

Most of the classical launch vehicle guidance algorithms rely on required velocity vector concept[8], which acts as basis for hit equation[6] to be solved in order to reach the desired target. Once this required velocity vector is calculated, the desired burnout position and burnout flight path angle are determined[9]. The innovative underlying concept of the proposed algorithm is performing an in-flight defined maneuver during the mid-course (after apogee i.e., decent phase) by keeping in view of the payload capabilities.

The duration of maneuver can be decided based on temporal or spatial means. If the duration of maneuver is based on time then the maneuver will be open loop form, because the time of flight of the vehicle will vary based on the propulsion characteristics, range, burnout conditions. If the duration of maneuver is a function of altitude/range then the maneuver will be in closed form, because the aim of the payload to impact the desired coordinates at the predefined altitude, irrespective of time. The predetermined maneuver can be any realizable function like sinusoidal, pulse, triangular, exponential, etc. as shown in Fig. 2. If the maneuver is of sinusoidal the variable parameters are maneuver amplitude and frequency, if the maneuver is pulse then the variable parameter is the pulse amplitude and if the maneuver is exponential then the variable parameter is the decay or rise slope of the maneuver. Maneuver can be executed by a variable or fixed thruster at center of gravity or close to center of gravity. Generic representation of the maneuver function is given below:

$$Z=F\,(a, f, y) \quad (1)$$

where

Z = Maneuver function

a = Amplitude of the considered maneuver function

f = Frequency of the considered maneuver function

y = Independent variable (time, altitude, downrange)

Values of the a & f are decided by the vehicle propulsive capability and the extent of dispersion planned and selection

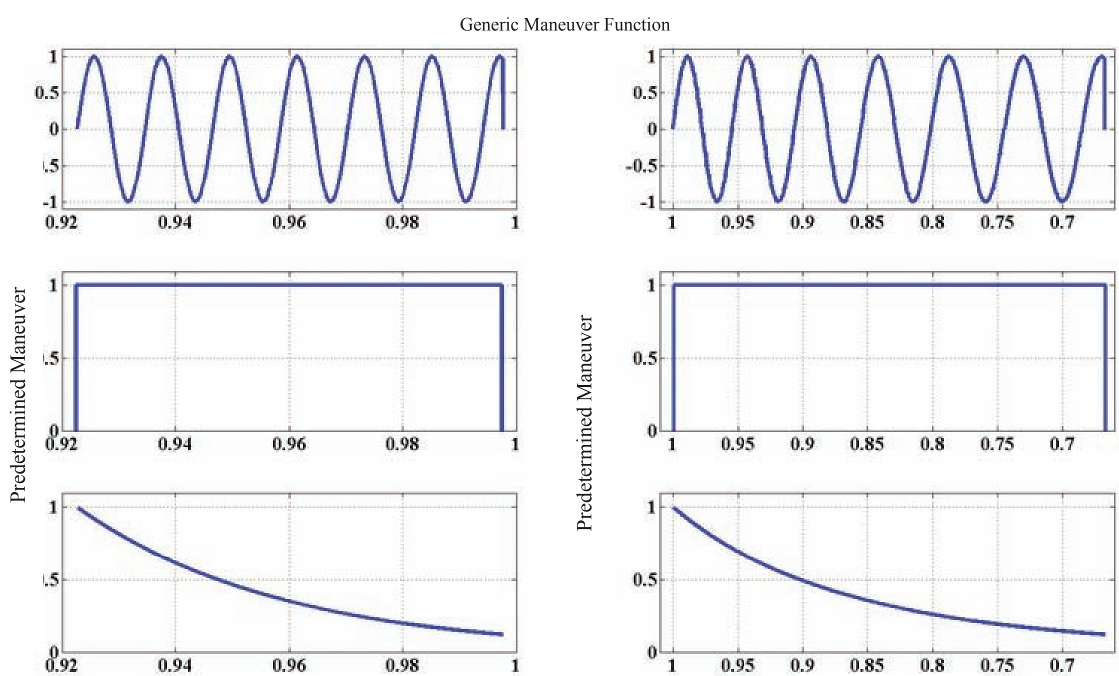

Figure 2. Predetermined maneuver functions as a function of normalized time and altitude.

of maneuver function can be random in selection but definite once selected. Once the determined maneuver initiation point, duration and the maneuver function is finalized, initiate the background simulation from the burnout point to the target. During the simulation, initiate the determined maneuver from the determined initiation point up to maneuver duration point (time, altitude). With this maneuver, compute the difference in the desired and achieved latitude and longitude at the impact point. Augment the ascent phase target coordinates with the above computed difference values in latitude and longitude and solve the hit equation (initiate the ascent phase guidance) with this augmented coordinates and repeat the above procedure till convergence criteria is met. Because of the mid-course maneuver there will be a change in the guidance solution (burnout conditions) to reach the desired target, which can be seen as the perturbation on the initial solution as shown below[7].

$$\frac{r_0}{a} = \frac{1-\cos(\phi+\Delta\phi)}{\lambda \sin^2\gamma} + \frac{\sin(\gamma-(\phi+\Delta\phi))}{\sin\gamma} \tag{2}$$

where

$r_0 = (a+h)$ = missile position from the center of the earth

a = equatorial radius (m), h = vehicle altitude from the surface of the earth

$\lambda = \frac{r_0 v^2}{GM}$ G = Universal gravitational constant

φ= range angle γ = flight path angle at burn out

$\Delta\phi$ = Augmented range angle corresponding to change in final coordinates

The steps involved in the proposed algorithm are given below:

(i) With the desired burnout state vector as the initial states, simulate the vehicle trajectory up to the desired predetermined altitude, from where determined maneuver is planned.

(ii) From predetermined altitude start of maneuver to the termination of the maneuver, superimpose a predetermined pseudo random maneuver (varying amplitude and frequency with altitude as the reference) to the actual attitude. During this maneuver period, activate thruster provided in the payload (typically called velocity package[10]) or side thrusters located at the center of gravity (if known accurately) can be used.

(iii) Once the predetermined attitude maneuver period completed, deactivate the thruster and simulate the vehicle trajectory up to the impact point. Note the achieved latitude and longitude.

(iv) Find the difference between the desired and achieved latitude and longitude, and augment the desired coordinates with this difference values.

(v) Repeat the steps from I to IV till the difference between the desired and achieved latitude and longitude lie within the desired tolerance bounds.

3. MATHEMATICAL MODELLING OF THE PAYLOAD VEHICLE

For the current work a standard nonlinear 6DoF mathematical model with 3 forces and 3 moments is considered[11]. In order to make the simulation more realistic a nonlinear aerodynamic model is considered, where the drag and aerodynamic forces are modeled as the functions of altitude, angle of attack and Mach number. The earth shape and rotational effects[12] are included in the simulation as the time of travel is variable which, if not accounted correctly, leads to tens of kilometers range errors[13]. A universal earth gravity model up to J2[14] term is considered to take care of earth gravitational effects, which is a function of colatitude and altitude.

Reentry atmospheric effects play a significant role during reentry, as the velocity with which the vehicle reenters is very high, in order to take care of this unwanted aerodynamic effects because of atmosphere, a more elaborate atmospheric model[15] is considered for simulation. In order to take care of wind effects during the reentry phase, a realistic wind model[16] is considered for studies. To assess the performance accurately a realistic inertial navigation model[17] is included in the simulation taking care of real time hardware features (accelerometer for acceleration, gyroscope for rate). A nonlinear reaction control system and liquid velocity package models are considered for the simulation studies.

$$\begin{bmatrix} \dot{u} \\ \dot{v} \\ \dot{w} \\ \dot{p} \\ \dot{q} \\ \dot{r} \end{bmatrix} = \begin{bmatrix} \left((T_{fx}-D_{fx})/m \right) - g_x \\ \left((T_{fy}-A_{fy})/m \right) - g_y \\ \left((T_{fz}-A_{fz})/m \right) - g_z \\ M_X / I_X \\ \left(M_y + (I_Z - I_X)pr\right)/I_y \\ \left(M_Z + (I_X - I_y)pq\right)/I_Z \end{bmatrix} \Rightarrow \dot{X} = f(X,U) \tag{3}$$

where u, v, w and p, q, r are translation and rotational components. T_{fx}, T_{fy}, T_{fz} and A_{fy}, A_{fz} are thrust and aerodynamic force components. D_{fx} is the drag force action along the body axial direction. m is the mass of the pay load, g_x, g_y, g_z are the gravitational components, and M_x, M_y, M_z and I_x, I_y, I_z are moment and inertia components respectively

For the present study, a 2 stage solid propelled launch vehicle with flex nozzle actuated control system is considered. Once the solid propelled stages are separated after propellent got consumed, the payload is controlled by using a reaction control system powered by liquid thrusters, enabling the flexibility of switching on and off when desired. During the ascent phase the vehicle follows a preprogrammed attitude turn keeping in view the initial constraints like structural load &control limitation, etc., Once the vehicle attains the desired relaxed conditions usually out of atmosphere, an explicit closed loop guidance[8] will guide and place the vehicle at burnout on a desired ellipse (function of burnout position, velocity, flight path angle &earth rotation rate compensated desired target position), by virtue of which the vehicles reaches the desired target. With these desired burnout state vector, a back ground

6DoF algorithm is initiated iteratively by using the proposed algorithm, till the 6DoF achieved impact latitude and longitude coincides with the desired one's as per the specified tolerance bounds.

4. SIMULATION RESULTS

To validate the proposed algorithm, different burnout conditions are considered for a given target as shown in Table 1. For the study a sinusoid (quaternion[18]) with an amplitude and frequency of 0.0001 Hz and 0.15 Hz is considered for determined attitude maneuver. Here it should be noted that the maneuver activation is based on altitude not on time, since the trajectory varies with burnout conditions and the guidance problem considered for simulation is a free time problem (i.e., the aim is to reach the target without any constraint on the time of flight). The input amplitude and frequency are same for all the three cases considered for simulation, but the trajectory parameters vary based on burnout conditions i.e., velocity, position, flight path angle, etc.

The thrust force can be provided by a small propulsion package with respect to altitude. During maneuver phase, a thruster with constant thrust force of 20 KN is considered. Once

Table 1. Different burnout conditions are considered for a given target

Case	State vector at the start of proposed algorithm (flight path angle, velocity & position)			Desired terminal conditions tolerence bound $\lvert\zeta\rvert \le 0.01^{\circ}$ (deg)		Achieved terminal conditions (without mid-course maneuver deception algorithm) deception trajectory (pseduo target) (deg)		Achieved terminal conditions (with mid-course maneuver deception algorithm) actual trajectory (actual target) (deg)	
	γ_{BO} (D)	V_{BO} (*m/s*)	P_{BO} (*m*)	Latitude	Longitude	Latitude	Longitude	Latitude	Longitude
1	13.85	4658	6514670	41.488637	87.088686	41.366969	87.115274	41.482585	87.090507
				(Desired -Achieved) Latitude & Longitude		0.121668	-0.026588	0.006051	-0.001821
2	16.07	4492	6519650	41.488637	87.088686	41.367018	87.111770	41.480964	87.088383
				(Desired -Achieved) Latitude & Longitude		0.121619	-0.023084	0.007672	0.000303
3	13.55	4612	6526009	41.488637	87.088686	41.395181	87.115627	41.496412	87.089302
				(Desired -Achieved) Latitude & Longitude		0.093455	-0.026941	-0.007775	-0.000616

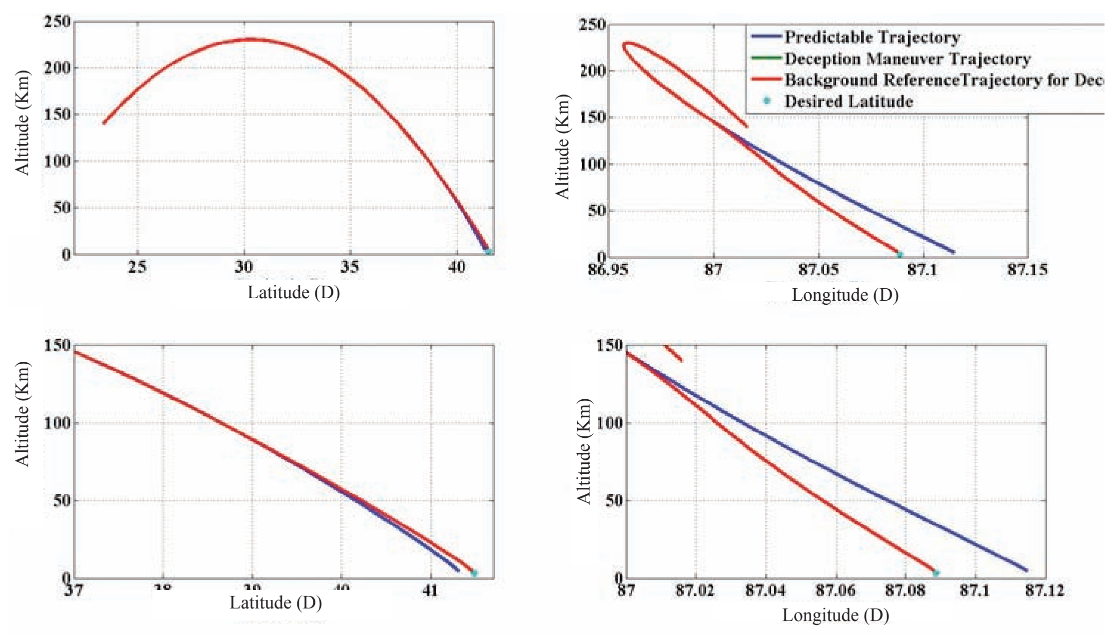

Figure 3. Case 1 Altitude *vs* latitude and longitude trajectory.

Note: The trajectory (final achieved coordinates) is sensitive to the burnout conditions and the band for burnout conditions considered for the simulation is selected considering some variations of solid propulsion.

the maneuver period is completed the thruster gets deactivated and the vehicle follows the ballistic path there after.

The execution of the determined maneuver for case 1 is shown in Fig. 3. The trajectory shown in blue color is the one which is generated by the payload without any deception maneuver and the green one is the one which is generated by the payload with a predetermined maneuver execution. From the Fig. 3 it is evident that the deception maneuver started at 150 km with a deviation from the predicted trajectory (blue trajectory). The trajectory shown in red colour is the background 6DoF trajectory which provides the reference for real time deception trajectory (green trajectory). The background and real time trajectory are in tight agreement because of which it is not possible to see the difference between red and green trajectory in the figure(s). Finally the realtime trajectory achieve's the desired latitude and longitude with in the given tolerance bounds. Figure 4 shows the altitude variation for with and without maneuver with respect to time. From the data markings in the figure, it is clear that the difference in the altitude between the non maneuvering and maneuvering trajectory is varying from 0 km to 9 km from 150 km altitude point to impact point. This magnitude can be increased by an additional impulse in the maneuvering vehicle.

The working of the algorithm for case 2 and case 3 are shown in Figs 5 and 6. Figures 5 and 6 shows the latitude and longitude variation with respect to altitude and it is clear from this figures that the algorithm drives the payload towards the desired target from the start of the deception point.

The robustness of the proposed algorithm under model uncertainty is studied by perturbing the wind, atmosphere

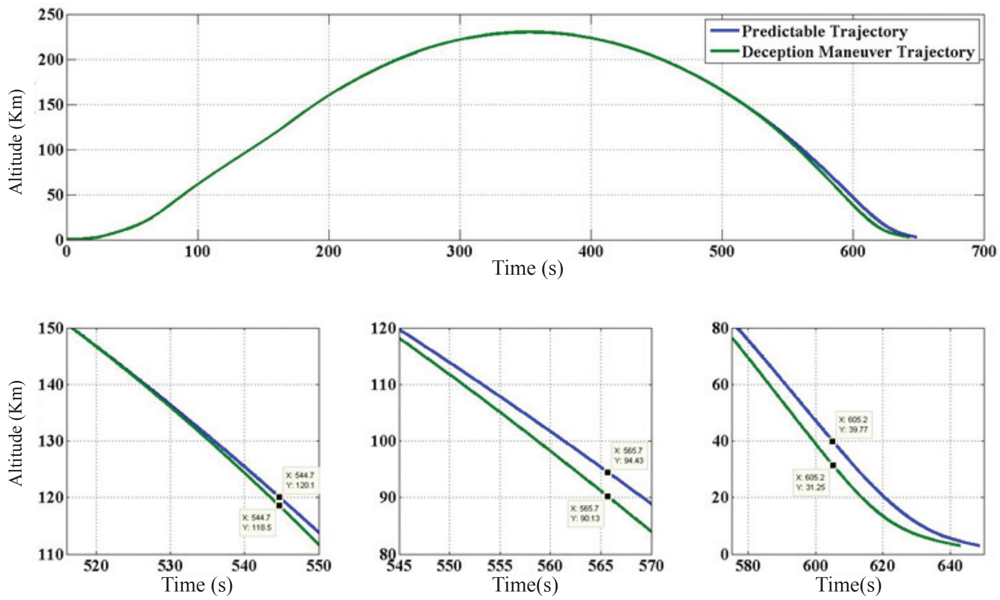

Figure 4. Case 1 : Time *vs* altitude.

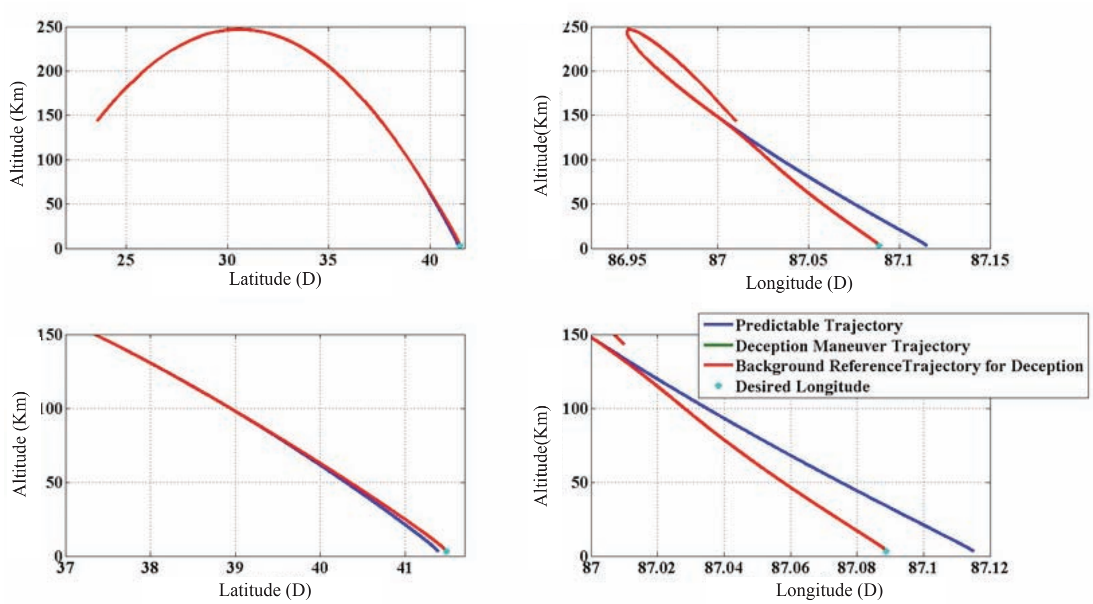

Figure 5. Case 2 : Altitude *vs* latitude and longitude trajectory.

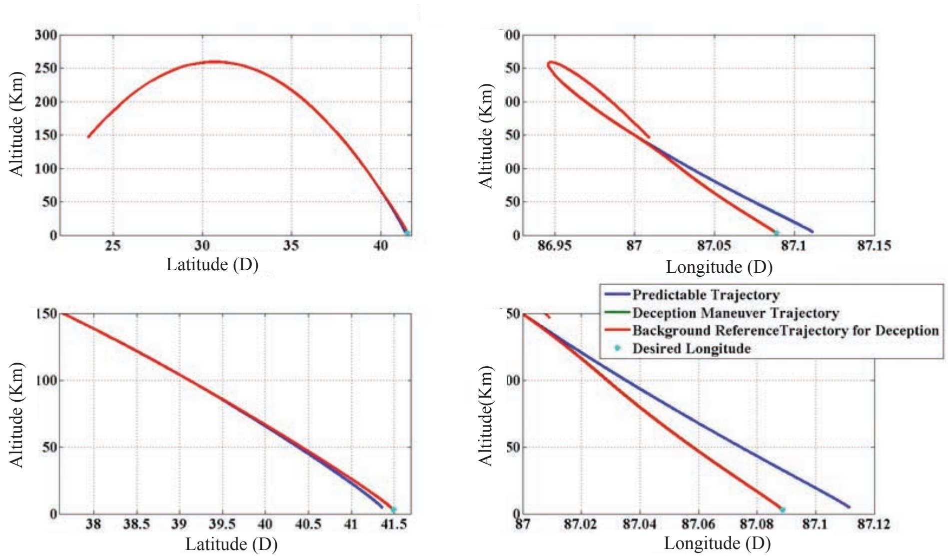

Figure 6. Case 3 : Altitude *vs* latitude and longitude trajectory.

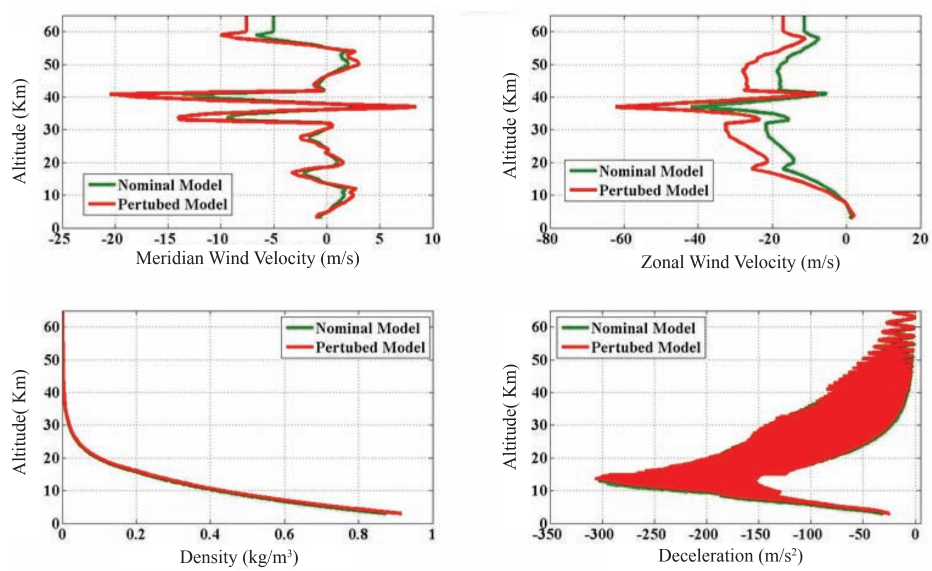

Figure 7. Case 4 : Altitude *vs* wind velocity, density and drag.

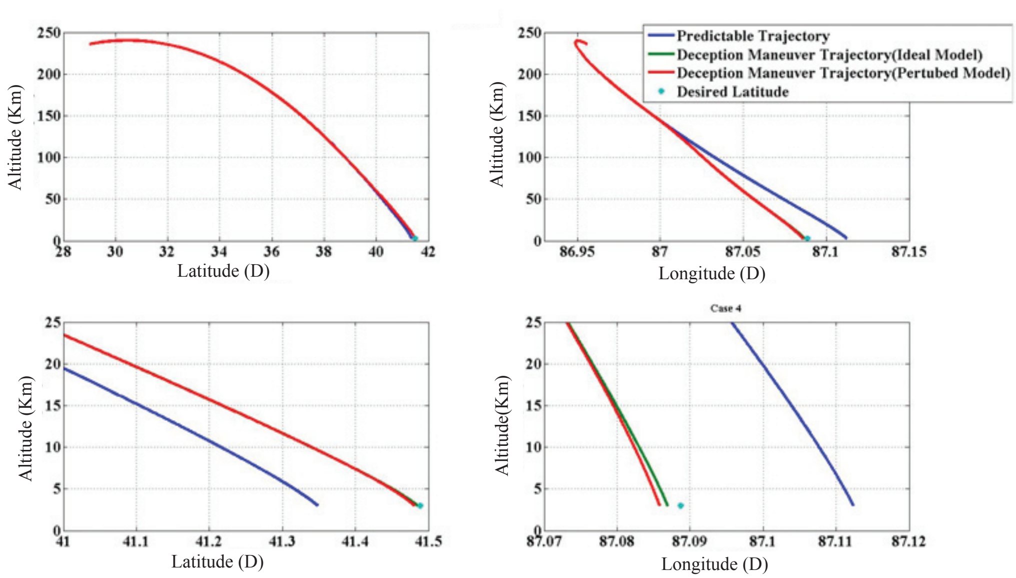

Figure 8. Case 4 : Altitude *vs* latitude and longitude.

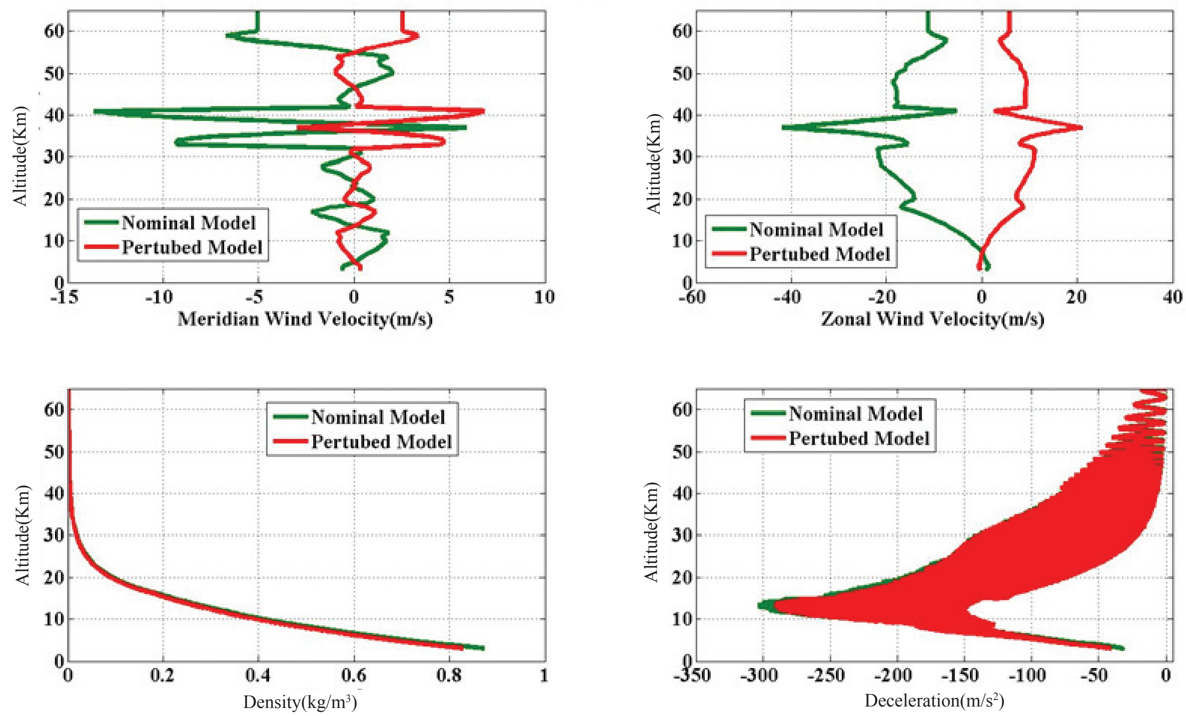

Figure 9. Case 5 : Altitude *vs* wind velocity, density, and drag.

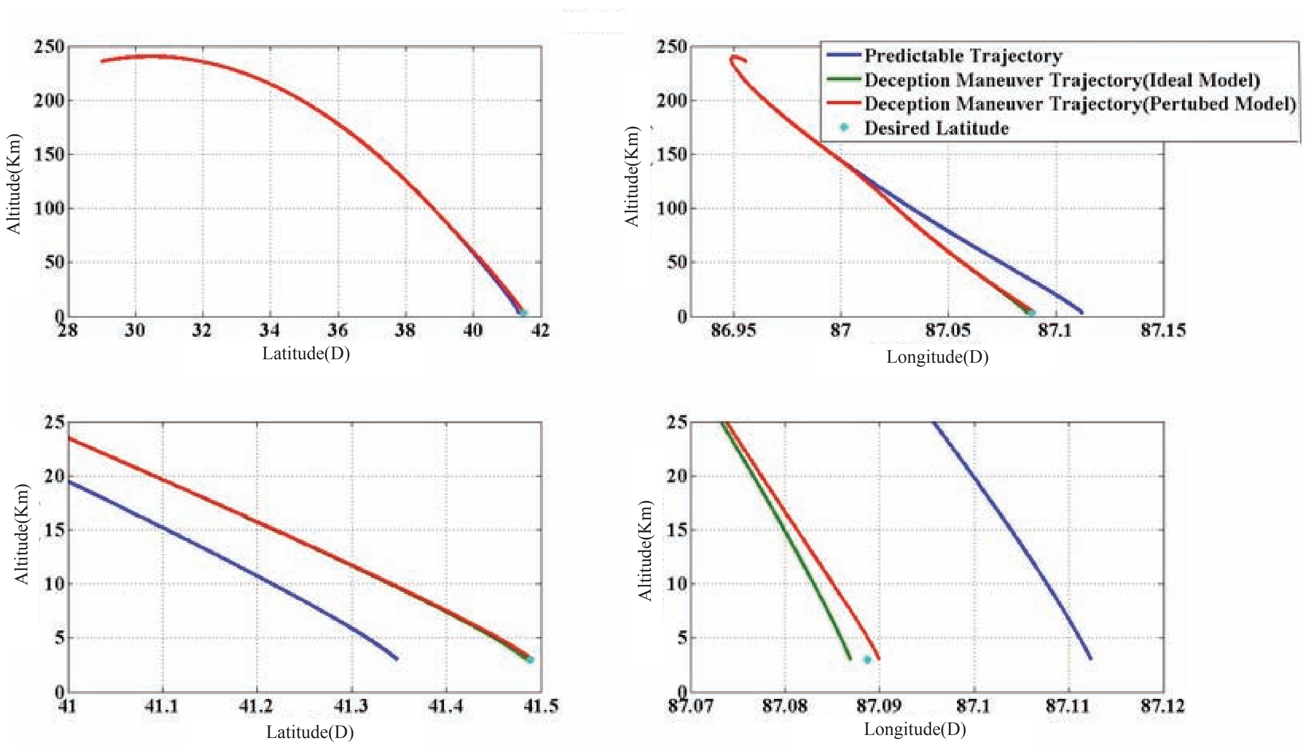

Figure 10. Case 5 : Altitude *vs* latitude and longitude.

Table 2. Perturbation bands considered for robustness studies

Case	Percentage of variation on the nominal wind, density and drag (assumed model)		
	Wind	Density	Drag coefficient
4	50	5	2
5	-50	-5	-2

Table 3. Burnout state vector considering for robustness studies

γ_{BO} (D)	V_{BO} (*m/s*)	P_{BO} (*m*)
13.85(D)	4658(m/s)	6514670(m)

Table 4. Robustness test case simulation results

Case	Desired terminal conditions (deg)		Achieved terminal conditions (without mid-course maneuver deception algorithm) pseudo target (deg)		Achieved terminal conditions (with ideal model mid-course maneuver deception algorithm) actual target (deg)		Achieved terminal conditions (with pertubed model mid-course maneuver deception algorithm) (deg)	
	Latitude	Longitude	Latitude	Longitude	Latitude	Longitude	Latitude	Longitude
4	41.488637	87.088686	41.348213	87.112340	41.485034	87.086906	41.480771	87.085815
	(Desired -Achieved) Latitude & Longitude		0.1404	-0.0237	0.0036	0.0018	0.0079	0.0029
5	41.488637	87.088686	41.348213	87.112340	41.485034	87.086906	41.491567	87.089976
	(Desired -Achieved) Latitude & Longitude		0.1404	-0.0237	0.0036	0.0018	-0.0029	-0.0013

and aero models. The case studies are listed in Table 2. The burnout state vector consider for the simulation studies shown in Table 3.

Table 4 shows the desired target point location, achieved terminal point location without (predictable trajectory) and with (deception trajectory) reentry maneuver.

Figure 7 & 9 shows the wind, atmospheric density and drag variation with respect to the altitude. The curves in green shows the model considered for background trajectory simulation, while the red one is considered for fore ground simulation. Figures 8 & 10 shows the latitude and longitude variation with respect to the altitude and it is clear from the figures that the final impact is achieved with in the prescribed tolerance bound, under model perturbations.

5. CONCLUSION

A practically working and implementable algorithm for real time mid-course maneuver with pre-corrected ascent phase guidance is described in the current paper. The work describes in detail the implementation of the deception maneuver and guidance algorithm by means of a 6DoF simulation from burnout point to impact. With the practicable available subsystem's the paper shows the robustness of the algorithm by means of some simulation cases by considering a wide band of burnout state vector values at the burnout. One of the flexibility of the proposed work is in selecting online the start and end point of maneuver with the variation of the amplitude and frequency of the maneuver, by keeping in view of the thrust force availability and capability. The present work can be extended to ascent phase guidance by virtue of which a wide band of dispersion at reentry can be taken care and it is also possible to use side thruster during the maneuver phase to decrease the payload response time for maneuver.

REFERENCES

1. George, N. Lewis & Theodore A. Postol, Defense and Arms Control Studies. Massachusetts Institute of Technology, Future Challenges to the Ballistic missile defense. *IEEE Spectrum*, 1997, **34(**9), 60-68.
2. Ran, Zhang; Huifeng, Li & Xudong, Cao. A new approach for re-entry vehicle trajectory planning and guidance, ICAS, 2012-5.7.5, **4**, pp. 3158-3164.
3. Changsheng, Gao; Wuxing, Jing; & Chaoyong, Li. Optimal guidance law design for reentry vehicle using virtual displacement concept. *In* the Proceedings of the 26th Chinese Control Conference, Zhangjiajie, Hunan, China, July 26-31, 2007, pp. 507-510.
4. Page, J.A. & Rogers, R.O. Guidance and control of maneuvering reentry vehicles, Decision and Control including the 16th Symposium on Adaptive Processes and a Special symposium on Fuzzy set theory and applications, 1977 IEEE Conference, Dec-1977, **16**, pp. 659-664.
5. Cameron, J.D.M. Explicit guidance equations for maneuvering reentry vehicles, re-entry and environmental systems divisions. General Electric Company, Philadelphia, Pa 19101, TP3-3:30.
6. George; R. & Pitman, Jr, Inertial Guidance. John Wiley & Sons, INC. Newyork, London, 1962.
7. Wheelon, Albert D. Free flight of a ballistic missile. *ARS Journal*, 1959, **29(**12), 915-926.
8. Siouris, George M. Missile guidance and control systems. Springer, 2004
9. Thomas, Tessy. Guidance scheme for solid propelled vehicle during atmospheric phase, *Def. Sci. J.*, 2005, **55(**3), 253-264.
10. Wilkey, John W. Velocity package. United States Patent No. 3,260,204. July 12, 1966.
11. Kadam, N.V. Practical design of flight control systems for launch vehicles and missiles. Allied Publishers Pvt Ltd. 2009.
12. Department of defence world geodetic system 1984. National Imagery and Mapping Agency, 3 January 2000.
13. Cornelisse, J.W.; Schoyer, H.F.R. & Wakker, K.F. Rocket propulsion and space flight dynamics. Pitman Publishing Limited, 1979.
14. Kenneth R. Britting, inertial navigation systems analysis, Wiley-Interscience, 1971.
15. Ananthasayanam, M.R. & Narasimha R. Standard

atmosphere for aerospace applications in India. Dept. of Aerospace Engg. Indian Institute of Science, Bangalore. Report No. 79 FM 5.
16. Narasimha, R. The wind environment in India. NAL. Technical Memorandum Du 8501, 1985.
17. Titterton, David & Weston, John. Strapdown inertial navigation technology, IET, 2nd Ed, 2004.
18. Kuipers, Jack B. Quaternions and rotation sequences. A primer with application to Orbits. Aerospace, and Virtual reality. Princeton University Press, Princeton, New Jersey. 2002.

Contributors

Mr Avinash Chander received his BE (Electrical Eng.) from IIT Delhi, in 1972 and MS (Spatial Information Technology) from Jawaharlal Nehru Technological University, Hyderabad. He is presently working as Distinguished Scientist in DRDO. He received many Awards like, *DRDO Scientist of the Year-1989, Astronautical Society of India Award-1997, DRDO AGNI Self reliance Award-1999, Dr Biren Roy Space award-2000, DRDO Award for Path Breaking Research/Outstanding Technology Development-2007, Outstanding Technologist Award-2008* by Punjab Technical University. His areas of interest include: Navigation, guidance, mission design.

Dr Iyyanki V. Murali Krishna received his MTech from IIT Madras and PhD from IISc, Bangalore in 1977. He is presently working as Director, Institute of Science and Technology and Coordinator of Centre for Atmospheric Sciences and Weather Modification Technologies at Jawaharlal Nehru Technological University, Hyderabad. His areas of interest includes: Geospatial technology and data mining, soft computing technologies, disaster management, satellite meteorology and weather informatics.